Extension of the Hybrid Scintillation Propagation Model to the Case of Field Propagation along the Magnetic Field

Vadim Gherm and Nikolay Zernov,

Department of Radiophysics

University of St.Petersburg, St.Petersburg, Russia

International Beacon Satellite Symposium BSS-2016
Trieste, Italy

HSPM - Hybrid Scintillation Propagation Model

Hybrid model for prediction of the field scintillation on transionospheric paths of propagation was developed as the combination of the complex phase method (CPM) and random screen technique.

V.E.Gherm, N.N.Zernov, and H.J.Strangeways, «Propagation model for transionospheric fluctuating paths of propagation: Simulator of the transionospheric channel», ***Radio Science***, ***40***, RS1003, doi:10.1029/2004RS003097, 2005.

Propagation from a satellite to the Earth's surface is calculated in two steps:

i) transversal spatial spectra of the field phase and log-amplitude are calculated by the complex phase method for the points of observations below the ionosphere. The spectra obtained are employed to generate a random realizations of the field composing a random screen below the ionosphere;

ii) the propagation problem for a random screen is rigorously solved to obtain the field's statistical moments and time series on the Earth's surface.

The random screen being introduced in the present method is a physical screen with log-amplitude and phase fluctuations relevant to a real field on a plane located below the ionosphere.

Anisotropy of the Ionospheric Turbulence

3D spatial spectra of fluctuations of the dielectric permittivity, which also depend on the slow spatial variable z along the path of propagation

$$\Phi_\varepsilon(\boldsymbol{\kappa}, \kappa_z, z) = a\sigma_N^2[1-\varepsilon_0(z)]^2 \frac{\Gamma(p/2)}{\Gamma((p-3)/2)} \frac{1}{\pi^{3/2}\kappa_0^3} \left(1 + \frac{\boldsymbol{\kappa}^2}{\kappa_0^2} + \frac{a^2\kappa_z^2}{\kappa_0^2}\right)^{-p/2}.$$

Here $a = l_\parallel / l_\perp$ is the aspect ratio with $l_\parallel$ and $l_\perp$ being the outer scales of turbulence along and across the magnetic field respectively, σ_N^2 is the variance of the fractional electron density fluctuation, $\varepsilon_0(z)$ is the permittivity of the ionosphere along the reference ray in z-direction, $\kappa_0 = 2\pi/l_\perp$, p is the spectral index.

2D spatial spectra of fluctuations

$$F_\varepsilon(\boldsymbol{\kappa}, \zeta, z) = \frac{\sigma_N^2[1-\varepsilon_0(z)]^2}{2^{(p-3)/2}\Gamma((p-3)/2)\pi\kappa_0^2} \left(\frac{\zeta\kappa_0}{a}\sqrt{1+\frac{\boldsymbol{\kappa}^2}{\kappa_0^2}}\right)^{\frac{(p-1)}{2}} K_{\frac{(p-1)}{2}}\left(\frac{\zeta\kappa_0}{a}\sqrt{1+\frac{\boldsymbol{\kappa}^2}{\kappa_0^2}}\right)\left(1+\frac{\boldsymbol{\kappa}^2}{\kappa_0^2}\right)^{-p/2}$$

The transversal spatial spectrum for log-amplitude fluctuations after passing the ionospheric layer

$$F_\chi(\boldsymbol{\kappa}, z) = \frac{k^2}{4}\int_0^z dz' \int_{-z_m(z')}^{z_m(z')} d\zeta \left\{\sin^2\left[\frac{\boldsymbol{\kappa}^2(z-z')}{2k}\right] - \sin^2\left[\frac{\boldsymbol{\kappa}^2\zeta}{4k}\right]\right\} F_\varepsilon(\boldsymbol{\kappa}, \zeta, z'). \qquad (1)$$

Here $F_\varepsilon(\boldsymbol{\kappa}, \zeta, z')$ is the two-dimensional spectrum of the permittivity fluctuations, $\boldsymbol{\kappa}$ is a two-dimensional transversal spectral variable (wave number). The integration limits are $z_m(z') = z - |2z' - z|$.

In the traditional treatment of the representation in equation (1), the second item is neglected. This is correct, if the irregularities are isotropic or are not fairly elongated.

$|\boldsymbol{\kappa}\zeta| < 2\pi\frac{l_\parallel}{l_\perp}$ $\quad \frac{|\boldsymbol{\kappa}|}{k} < \frac{\lambda}{l_{min\perp}} \ll 1$ $\quad$ then $\left|\frac{\boldsymbol{\kappa}^2\zeta}{4k}\right| < \frac{\pi}{2}\frac{l_\parallel}{l_\perp}\frac{\lambda}{l_{min\perp}}$ and may not be negligible if $\frac{l_\parallel}{l_\perp} \gg 1$.

The effective domain of integration in ζ is defined by the inequality $|\boldsymbol{\kappa}\zeta| < 2\pi\frac{l_\parallel}{l_\perp}$, since F_ε vanishes outside.

If the values of $\boldsymbol{\kappa}$ satisfy the inequality $|\boldsymbol{\kappa}|z \gg l_\parallel/l_\perp$ then $|\zeta| \ll z$ and $z_m \to \infty$

1. $z_m \to \infty$

After integration over ζ

$$F_{\chi,S}(\boldsymbol{\kappa}, z) = \frac{\pi k^2}{4} \int_0^z dz' \left\{ \frac{1}{2} \Phi_\varepsilon \left(\boldsymbol{\kappa}, \frac{\boldsymbol{\kappa}^2}{2k}, z' \right) + \frac{1}{2} \Phi_\varepsilon \left(\boldsymbol{\kappa}, -\frac{\boldsymbol{\kappa}^2}{2k}, z' \right) \mp \Phi_\varepsilon(\boldsymbol{\kappa}, 0, z') \cos \left[\frac{\boldsymbol{\kappa}^2 (z - z')}{k} \right] \right\}, \qquad (2)$$

Instead of the traditional one

$$F_{\chi,S}(\boldsymbol{\kappa}, z) = \frac{\pi k^2}{4} \int_0^z dz' \Phi_\varepsilon(\boldsymbol{\kappa}, 0, z') \left\{ 1 \mp \cos \left[\frac{\boldsymbol{\kappa}^2 (z - z')}{k} \right] \right\}. \qquad (3)$$

2. for small $|\boldsymbol{\kappa}|$ $F_\chi(\boldsymbol{\kappa}, z)$ is negligibly small, and

$$F_S(\boldsymbol{\kappa}, z) = \frac{k^2}{4} \int_0^z dz' \int_{-z_m(z')}^{z_m(z')} d\zeta \, F_\varepsilon(\boldsymbol{\kappa}, \zeta, z'). \qquad (4)$$

The integration should be carried out in finite limits $z_m(z') = z - |2z' - z|$

Spectra of log-amplitude and phase after passing the ionospheric layer

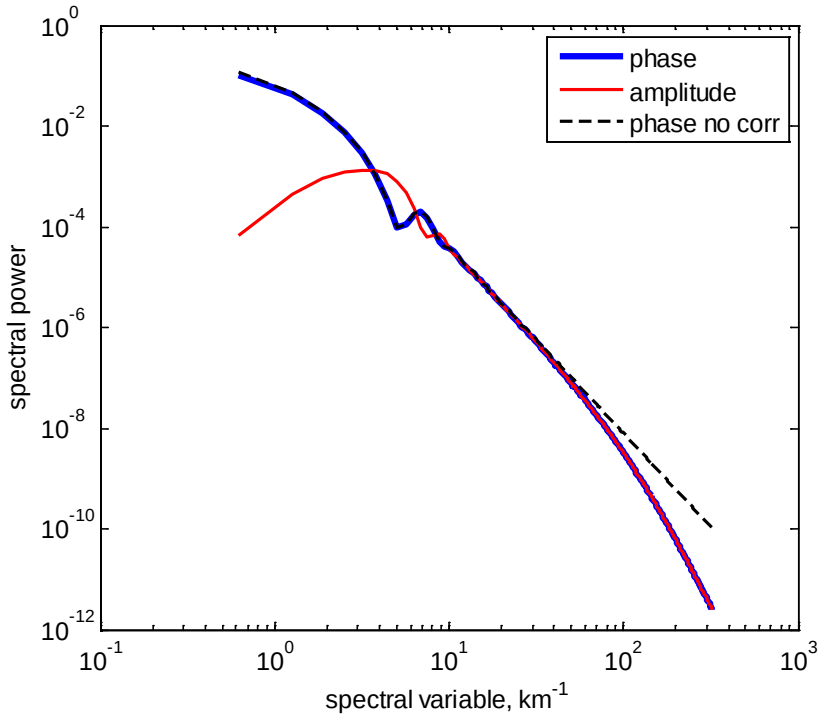

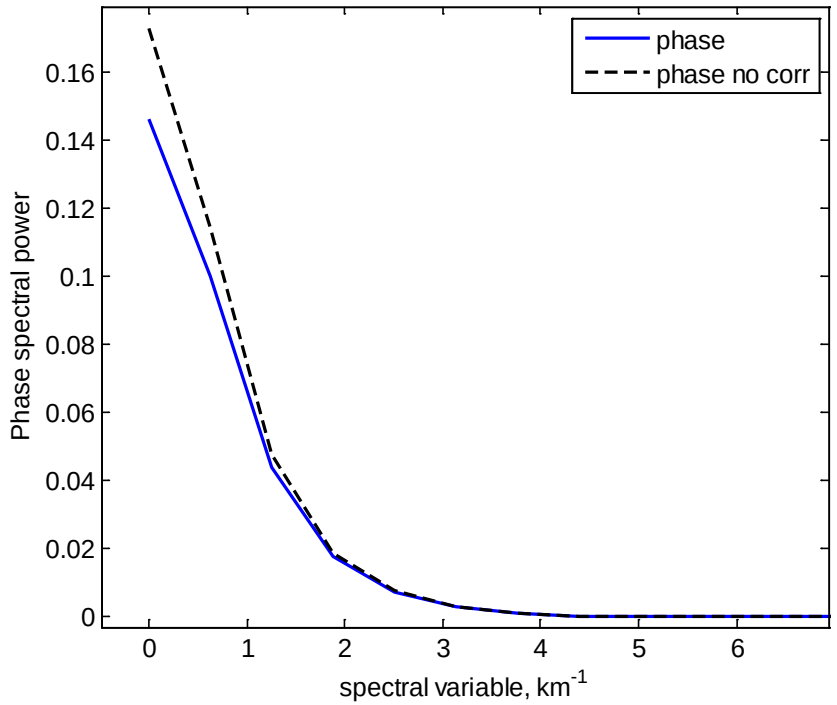

On the left: one-dimensional cuts of 2-D spectra of log-amplitude (red), and phase (blue) obtained utilizing (2) and (4). The black dot curve is the classical phase spectrum without corrections. On the right: the large-scale part of the phase spectra is plotted in linear scale

parameters: $l_{\perp}$=5 km, a=50, p=3.7, f=150 MHz.

Spectra of amplitude and phase on the Earth.
Dependence on the angle Ψ between ray path and magnetic field direction.

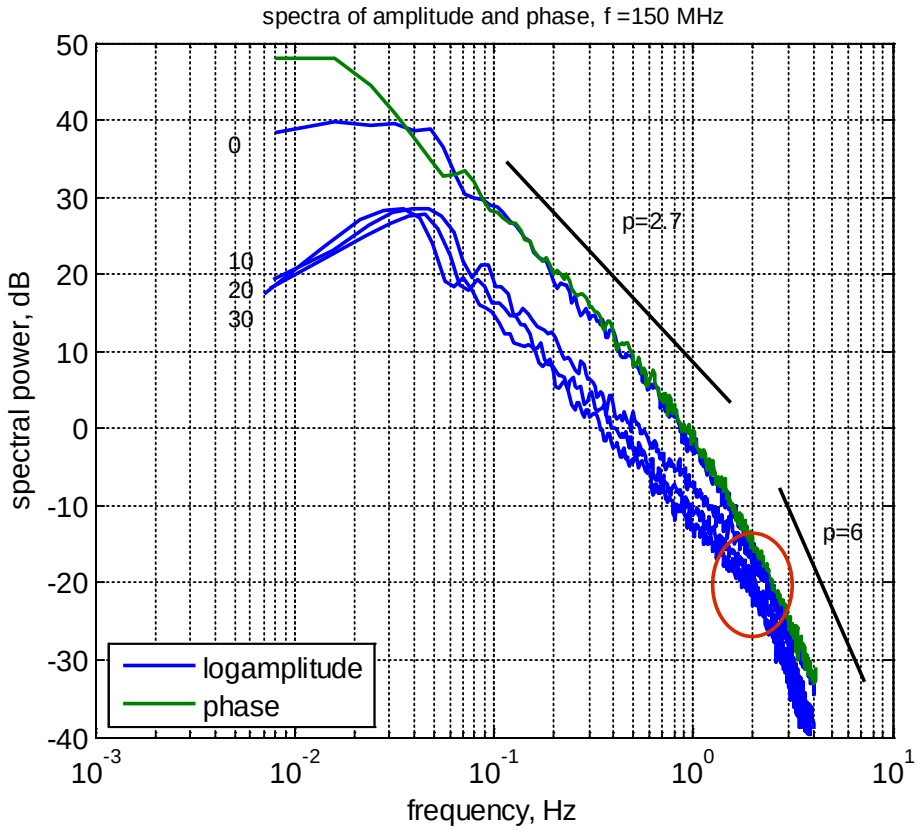

a=50 L0=5 sigmaN= 0.0005
TEC=52

Dependence on the Ψ

Ψ=0° S4=0.42
Ψ=10° S4=0.11
Ψ=20° S4=0.09
Ψ=30° S4=0.086

Spectra of amplitude and phase on the Earth. Dependence on the anisotropy (aspect ratio a).

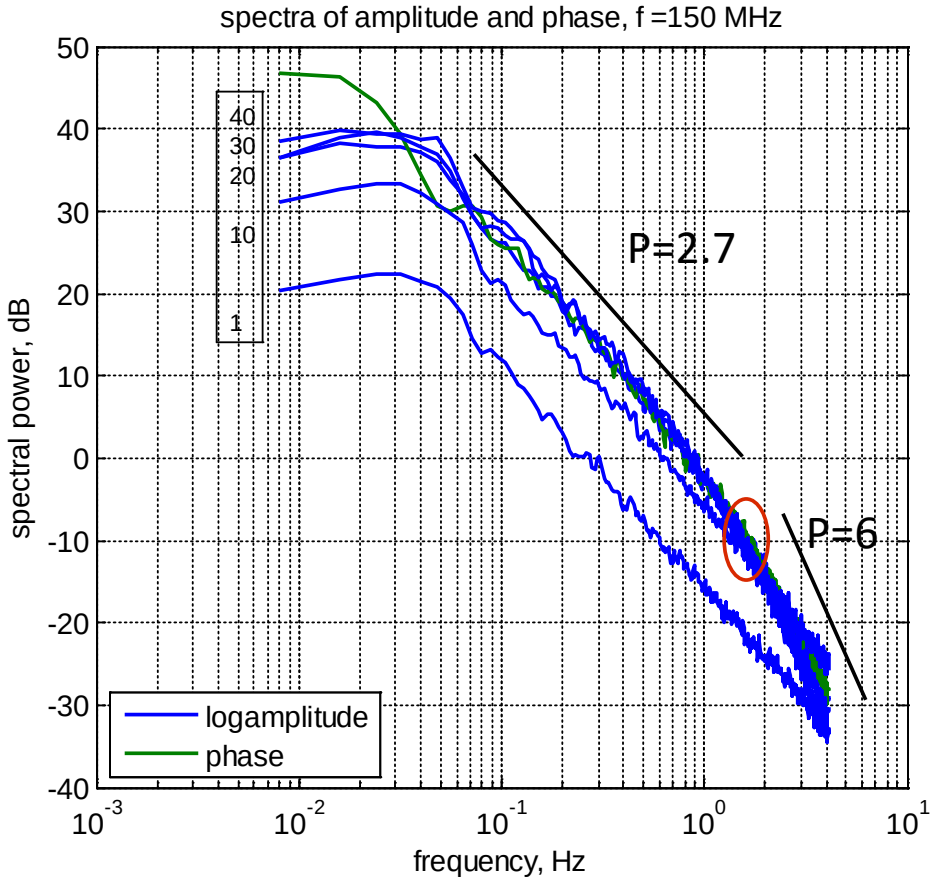

el=60° L0=5 (ψ=0°)

Dependence on anisotropy
a=50 (S4= 0.42)
a=40 (S4= 0.37)
a=30 (S4= 0.32)
a=20 (S4= 0.26)
a=10 (S4= 0.18)
a=1 (S4= 0.057)

Experimentally measured VHF intensity fluctuations spectra

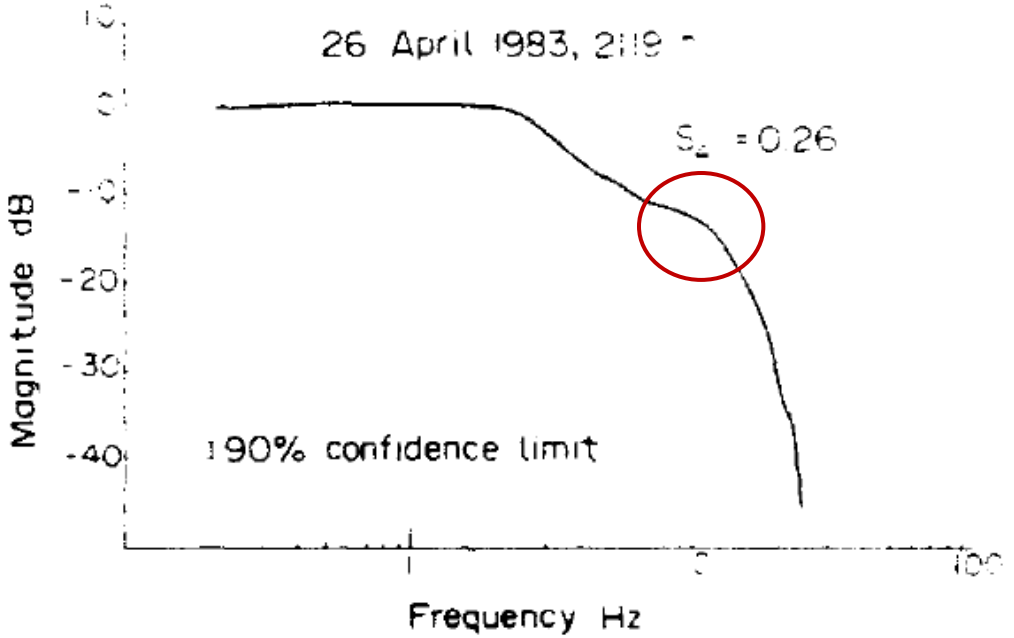

Fig. 6. An example of a power spectrum showing a break in slope at around 10 Hz, obtained on 26 April 1983 at 2119 UT.

Kersley, H. Chandra, Power spectra of VHF intensity scintillations from F2- and E-region ionospheric irregularities, Journal of Atmospheric and Terrestrial Physics, Volume 46, Issue 8, 1984, Pages 667-672

Experimentally measured VHF phase fluctuations spectra

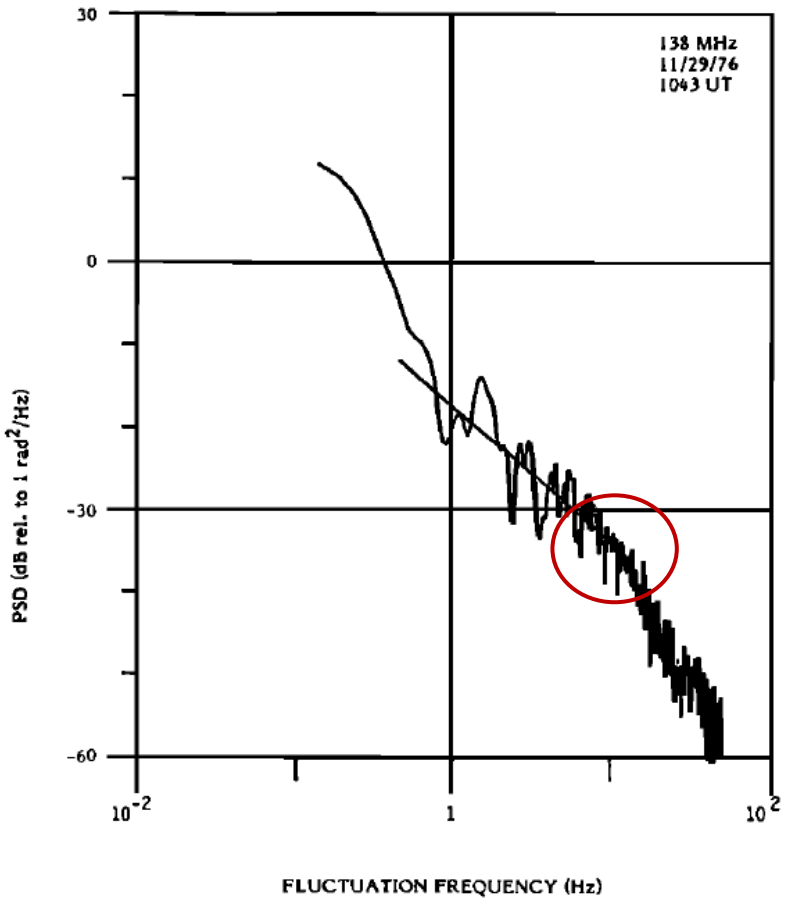

Fig. 5. VHF phase spectrum displaying a high-frequency downward break as well as the low-frequency upward (inverse) break noted in the two spectra of Figure 4.

Fremouw, E. J., J. A. Secan, and J. M. Lansinger (1985), Spectral behavior of phase scintillation in the nighttime auroral region, Radio Sci., 20(4), 923–933, doi:10.1029/RS020i004p00923

Simulated VHF signal fluctuations spectra

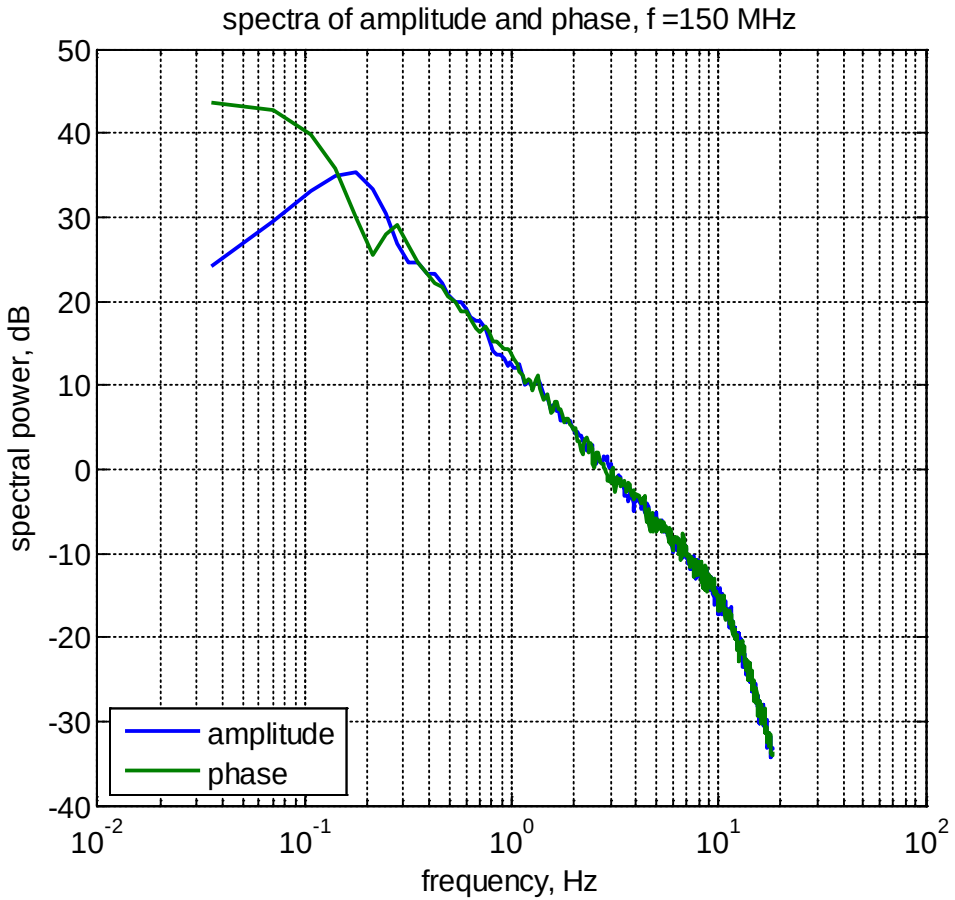

a=30°
Ψ=30°
Vd=500 m/c
S4=0.2

Conclusions

- The case of transionospheric propagation in the direction of magnetic field in fairly anisotropic fluctuating ionosphere has been considered aiming at the proper treatment of the anisotropy effects.
- The Hybrid Scintillation Propagation Model has been modified incorporating the more general formulas obtained.
- The results of VHF propagation simulations show that the spectra of phase and amplitude fluctuations deviate from the pure power law in their high frequency part.
- This may be interpreted as a “spectral brake”, or as the “two-slope” power law with no corresponding break in the spectrum of the electron density fluctuations.
- This effect is exclusively due to the diffraction in the volume. It cannot be obtained in frames of the phase screen and MPS techniques, as well as in the Markov parabolic equations approach.